Original Article

Collagen immobilization on ultra-thin nanofiber membrane to promote *in vitro* endothelial monolayer formation

Byeong-ung Park[1,2],* 🆔, **Sang Min Park[3,4],*, Kyoung-pil Lee[1,2],**
Seong Jin Lee[3], Yu Eun Nam[1,2], Han Sang Park[2], Seongsu Eom[3],
Jeong Ok Lim[5], Dong Sung Kim[3] and Hong Kyun Kim[1,2]

Abstract

The endothelialization on the poly (ε-caprolactone) nanofiber has been limited due to its low hydrophilicity. The aim of this study was to immobilize collagen on an ultra-thin poly (ε-caprolactone) nanofiber membrane without altering the nanofiber structure and maintaining the endothelial cell homeostasis on it. We immobilized collagen on the poly (ε-caprolactone) nanofiber using hydrolysis by NaOH treatment and 1-ethyl-3-(3-dimethylaminopropyl) carbodiimide/sulfo-*N*-hydroxysulfosuccinimide reaction as a cost-effective and stable approach. NaOH was first applied to render the poly (ε-caprolactone) nanofiber hydrophilic. Subsequently, collagen was immobilized on the surface of the poly (ε-caprolactone) nanofibers using 1-ethyl-3-(3-dimethylaminopropyl) carbodiimide/sulfo-*N*-hydroxysulfosuccinimide. Scanning electron microscopy, Fourier transform infrared spectroscopy, transmission electron microscopy, and fluorescence microscopy were used to verify stable collagen immobilization on the surface of the poly (ε-caprolactone) nanofibers and the maintenance of the original structure of poly (ε-caprolactone) nanofibers. Furthermore, human endothelial cells were cultured on the collagen-immobilized poly (ε-caprolactone) nanofiber membrane and expressed tight junction proteins with the increase in transendothelial electrical resistance, which demonstrated the maintenance of the endothelial cell homeostasis on the collagen-immobilized-poly (ε-caprolactone) nanofiber membrane. Thus, we expected that this process would be promising for maintaining cell homeostasis on the ultra-thin poly (ε-caprolactone) nanofiber scaffolds.

Keywords

Tissue engineering, nanofiber membrane, collagen, biomimetic model, post-processing

Introduction

Tissue engineering has been reported to be useful for regenerative medicine[1,2] and organ replacement therapy for the cutaneous,[3,4] neural,[5,6] ophthalmic,[7] cardiovascular,[8–10] pulmonary,[11,12] and skeletal (bone and cartilage) systems,[13–15] and also for testing the efficacies of new drugs in *in vitro* cell culture platforms.[16–20] For applications in these fields, scaffolds of biomimetic microstructures have been developed that can reproduce specific functions of the native organ by mimicking *in vivo* cellular microenvironments. One of the challenges in

[1]Bio-Medical Institute, Kyungpook National University Hospital
 (KNUH), Daegu, South Korea
[2]Department of Ophthalmology, School of Medicine, Kyungpook
 National University, Daegu, South Korea
[3]Department of Mechanical Engineering, Pohang University of Science
 and Technology (POSTECH), Pohang, South Korea
[4]School of Mechanical Engineering, Pusan National University, Busan,
 South Korea
[5]Biomedical Research Institute, Joint Institute for Regenerative
 Medicine, School of Medicine, Kyungpook National University,
 Kyungpook National University Hospital, Daegu, South Korea

*These authors contributed equally to this work

Corresponding authors:
Hong Kyun Kim, Bio-Medical Institute, Kyungpook National University
Hospital (KNUH), 680 Gukchaebosang-ro, Jung-gu, Daegu 41944,
South Korea.
Email: okeye@knu.ac.kr

Dong Sung Kim, Department of Mechanical Engineering, Pohang
University of Science and Technology (POSTECH), 77 Cheongam-Ro,
Nam-Gu, Pohang 37673, Gyeongbuk, South Korea.
Email: smkds@postech.ac.kr

tissue engineering is to reproduce blood vessels as they exist in most organs. Blood vessels, which are lined by endothelial cells, perform a wide range of complex functions such as cellular and biochemical transport, nutrient and oxygen exchange, and temperature regulation.[21] Malfunctions and regulatory disturbances of blood vessels can cause serious problems such as Alzheimer's disease, hypertension, cardiac arrest, stroke, heart failure, dementia, and peripheral artery disease.[22] Thus, many researchers have focused on developing scaffolds that can effectively reproduce a blood vessel for regenerative medicine and drug discovery.[23–25]

As *in vivo* cellular microenvironments are mainly composed of collagen nanofibrils,[26] several research groups have attempted to fabricate scaffolds composed of nanofibers.[27] Among various nanofiber fabrication techniques, electrospinning is considered a simple and versatile tool for producing nanofiber scaffolds for tissue engineering because of its ability to mimic the structure of the native extracellular matrix (ECM).[26,28,29] In addition, the nanofibers have the potential to increase cell adhesion by providing a wider surface area and improving the cell–material and cell–cell interaction.[30,31] With these benefits, electrospun nanofiber scaffolds such as the tubular conduit[23] and mesh[32] have been developed to reconstruct blood vessels. The materials for electrospun nanofiber scaffold varied from natural to synthetic polymers. Compared to the natural polymer, electrospun nanofibers composed of synthetic polymers such as poly (ε-caprolactone) (PCL), poly (lactide) (PLA), poly (glycolic acid) (PGA), and poly (D, L-lactide-*co*-glycolide) (PLGA) possess better properties for tissue engineering of blood vessel in terms of biodegradability, mechanical strength, and cost-effectiveness. In addition, the mechanical properties and rate of degradation of the synthetic polymers can be regulated.[33,34] However, the synthetic polymers are often hydrophobic, which may induce non-native conformation of protein, thereby suppressing the bioactivity including cell attachment, viability, and proliferation.[35] To increase cell adhesion, post-processing techniques such as plasma treatment, wet chemical method, surface graft polymerization, and co-electrospinning of surface active agents and polymers have been developed for the electrospun synthetic nanofibers.[36] Among them, the wet chemical methods, including hydrolysis, aminolysis, and wet coating, generally provided a low cost, simple and stable approach to functionalize the synthetic polymers without requiring expensive equipment.

The objective of this study was to fabricate a collagen-immobilized ultra-thin PCL nanofiber membrane in a low cost and stable way with preserving the nanofiber structure, and maintain the endothelial cell homeostasis on it. This study reported a wet chemical method of hydrolysis, followed by the 1-ethyl-3-(3-dimethylaminopropyl) carbodiimide (EDC)/*N*-hydroxysulfosuccinimide (sulfo-NHS) reaction, for immobilizing collagen on the surface of the PCL nanofibers and promoting endothelialization. Considering the utility of nanofiber scaffolds in *in vitro*

cell culture platforms such as a Transwell® insert and an organ-on-a-chip, we fabricated a PCL nanofiber scaffold in the form of an ultra-thin, free-standing nanofiber membrane, which was intended to mimic an *in vivo* blood vessel-tissue interface. Previously, we have shown that the Matrigel coating on the ultra-thin PCL nanofiber membrane after plasma treatment, fabricated using an electrolyte-assisted electrospinning process, reproduced an *in vitro* multi-layered blood vessel/tissue interface, which enabled investigation on leukocyte infiltration through the blood vessel *in vitro*.[37,38] In this study, we utilized the wet chemical method based on hydrolysis, followed by EDC/sulfo-NHS reaction, as a cost-effective method for surface modification by stably bonding collagen on the surface of PCL nanofibers, producing a collagen-immobilized PCL (COL-PCL) nanofiber membrane. Collagen immobilization on the ultra-thin PCL nanofiber membrane was confirmed using scanning electron microscopy (SEM), fluorescence microscopy, Fourier transform infrared spectroscopy (FTIR), and transmission electron microscopy (TEM). Human umbilical vein endothelial cells (HUVEC) were cultured to form the endothelium on the COL-PCL nanofiber membrane and maintain endothelial cell homeostasis, recapitulating the barrier function of native blood vessels.

Materials and methods

Fabrication of ultra-thin PCL nanofiber membrane using electrospinning

To fabricate PCL nanofiber membranes, PCL ($M_n = 80,000$ g mol)$^{-1}$, methanol, and chloroform were purchased from Sigma-Aldrich (USA). A 7.5% PCL solution was prepared by dissolving PCL pellets in a mixture of methanol and chloroform (1:3, v/v). The PCL solution was filled in a syringe and ejected through a 23-gauge metal needle using a syringe pump (KDS200, KD Scientific, USA) at a constant flow rate of 0.5 mL h.$^{-1}$ A custom-made collector with two parallel stainless steel plates was placed approximately 20 cm apart from the tip of the metal needle. An ultra-thin PCL nanofiber membrane was fabricated in an environmentally controlled chamber using a high-voltage supplier (HV30, NanoNC, Korea) by applying an electrical voltage of 19 kV between the metal needle and the collector. The ultra-thin PCL nanofiber membrane was detoxified by placing it in a vacuum chamber for 24 h, and then transferred to a custom-made 24-well insert, which originally contained no porous membrane. The growth surface area of custom-made 24-well insert is 0.33 cm^2.

Surface immobilization of collagen on ultra-thin PCL nanofiber membrane

The fabricated ultra-thin PCL nanofiber membrane was treated with 0.1 M sodium hydroxide (NaOH) at room temperature

for 1 h to render it hydrophilic, followed by three rinses with deionized (DI) water. The PCL nanofiber membrane was then incubated in a 100 mM EDC and 100 mM sulfo-NHS solution (ratio of 1:1, v/v) in a 0.625 M 2-(N-morpholino) ethanesulfonic acid (MES) (pH 6.0) buffer for 2 h at room temperature. Subsequently, 2 mg mL^{-1} collagen type I from rat tail (Corning, USA) in 0.625 M MES buffer (pH 6.0) was immobilized on the surface of the PCL nanofibers at 37°C for 1 h in a humid chamber. After completion of the immobilization of collagen type I, the PCL nanofiber membrane with the collagen solution in 0.625 M MES buffer was washed thrice with 1× phosphate-buffered saline (PBS). A 0.1 M sodium phosphate solution was added and reacted for 2 h at room temperature for neutralizing the acid. Finally, the sodium phosphate solution was rinsed using DI water to obtain ultra-thin COL-PCL nanofiber membrane.

Characterization of ultra-thin nanofiber membranes

Field-emission scanning electron microscopy (SEM; SU6600, Hitachi, Japan) was employed to assess the fabricated electrospun PCL and COL-PCL nanofibers. The diameter of the nanofibers was determined from the SEM images using Image J (National Institutes of Health, USA). To measure the thickness of the ultra-thin PCL and COL-PCL nanofiber membranes, the latter were fixed in polydimethylsiloxane (PDMS) by pouring a mixture of PDMS monomer and curing agent (Dow Corning, USA) at a weight ratio of 10:1 and baking under 50°C for 24 h. The thickness of the nanofiber membrane was determined from the cross-sectional image of the nanofiber membrane-embedded PDMS.

The water contact angles of the PCL and COL-PCL nanofiber membranes were measured using a contact angle measurement instrument (SmartDrop, Femtobiomed, Korea). Five microliters of DI water were dropped onto the PCL and COL-PCL nanofiber membranes to evaluate their wettability.

Aniline blue staining

To confirm the presence of the collagen, we performed the staining of the collagen in the PCL and COL-PCL nanofiber membrane using aniline blue staining. Aniline blue solution was prepared by adding 2.5 g aniline blue and 2 mL acetic acid in 100 mL DI water. The samples were stained by socking in aniline blue solution for 10 min at room temperature. After 10 min later, aniline blue solution was suctioned and washed three times with DI water. Aniline blue-stained collagen on the PCL nanofiber was visualized using optical microscopy.

Fourier-transform infrared spectroscopy

The chemical structures of the PCL, NaOH-treated PCL, EDC/sulfo-NHS-treated PCL, physically collagen-adsorbed PCL (P-COL-PCL) and COL-PCL nanofiber membrane were characterized using a Fourier transform infrared (FTIR) spectrophotometer (Vertex 70, Bruker, Germany). The physically collagen-adsorbed PCL nanofiber membrane was prepared by coating collagen solution at the concentration of 5 μg cm^{-2} and incubating at room temperature for 1 h. After that, the collagen solution was removed and washed with 1× PBS. The COL-PCL nanofiber membrane was rinsed with DI water and dehydrated with a graded ethanol series (30%, 50%, 70%, 90%, and 100%). Subsequently, the COL-PCL nanofiber membrane was lyophilized using a freeze-dryer. An average of 64 scans in a range from 4000 to 500 cm^{-1} with a resolution of 4 cm^{-1} was conducted for each sample.

Field Emission transmission electron microscope (FE-TEM)

To confirm the immobilized collagen on the PCL nanofiber, the morphology of the PCL, P-COL-PCL, and COL-PCL nanofiber membrane was examined by transmission electron microscopy (TEM, HT7700, Hitachi, Japan). All samples were completely dried for TEM observation. The samples were placed on a copper grid and observed by TEM at ×4500 magnification.

Cultivation of HUVECs

HUVECs were purchased from Promocell (Germany) and cultured on collagen type I-coated cell culture dish (Corning, USA) containing endothelial basal medium (EBM-2, Lonza, Switzerland) with Single Quotes kit supplement (Lonza, Switzerland) at 37°C in a humidified 5% CO_2 atmosphere. The medium was changed after every 48 h until the cells reached 80% confluence. The HUVECs were cultured up to passage 8 in EBM-2 with Single Quotes kit supplement. The cells were stored at −80°C for further study.

Cell viability and permeability assays

The HUVECs were seeded onto the ultra-thin PCL, P-COL-PCL and COL-PCL nanofiber membranes at a density 2 × 10^5 cells/insert and cultured for 7 days. After culturing, the cells were rinsed with 1× PBS and then stained with ethidium homodimer-1 and calcein AM (live/dead® viability/cytotoxicity kit, Molecular Probes, USA) to confirm cell viability on the PCL, P-COL-PCL and COL-PCL nanofiber membranes.

A permeability assay was performed on the PCL, P-COL-PCL and COL-PCL nanofiber membranes, each of which was integrated on a custom-made 24-well insert. One hundred microliters of 2 mg mL^{-1} 40 kDa FITC-dextran (Sigma, USA) was added to the apical side of the 24-well insert with the nanofiber membrane, while 600 μL Hank's balanced salt solution (HBSS) was added to the

basal side of the insert. The area of the nanofiber membrane was 0.33 cm^2. The permeability assay was conducted at 37C for 1 h. The fluorescence intensity of the 40 kDa FITC-dextran at the basal side was measured using a microplate reader (BioTek, USA). The permeability coefficient was calculated as follows

$$P = \frac{dQ}{dt} \times \frac{1}{C_0 A} \qquad (1)$$

where dQ/dt is the mass transport rate of the 40 kDa FITC-dextran, C_0 is the initial concentration of 40 kDa FITC-dextran, and A is the area of the nanofiber membrane.

Measurement of transendothelial electrical resistance

The transendothelial electrical resistance (TEER) values of the HUVECs cultured on the ultra-thin PCL, P-COL-PCL and COL-PCL nanofiber membranes integrated on the custom-made 24-well inserts were measured daily for 7 days using a commercially available TEER measurement device (EVOM2, World Precision Instruments, USA) and the chopstick electrode set (STX3, World Precision Instruments, USA) per the guidelines of the EVOM2 instruction manual. The electrical resistance values of the HUVEC layers on the PCL, P-COL-PCL and COL-PCL nanofiber membranes were subtracted from those of the original PCL, P-COL-PCL and COL-PCL nanofiber membranes in the absence of HUVECs, respectively, and the subtracted values were multiplied by the area of the PCL, P-COL-PCL and COL-PCL nanofiber membranes to obtain the final TEER values of the HUVEC layers.

Immunofluorescence microscopy

The samples were fixed with 4% paraformaldehyde for 10 min at room temperature after 7 days of culturing. The fixed samples were washed with 1× PBS for 30 min and then blocked with 0.2% normal goat serum and 0.2% Triton X-100 in PBS for 1 h at room temperature. Immunofluorescence was performed with the following antibodies: rabbit anti-CD31/PE-CAM (Novusbio, USA, 1:50), rabbit anti-VE-cadherin (Cell Signaling Technology, USA, 1:50), mouse anti-Zo-1 (ThermoFisher Scientific, USA, 1:50), and mouse anti-claudin 5 (Abcam, England, 1:50). The samples were incubated with the primary antibodies at room temperature for 1 h and then washed thrice with 1× PBS. Alexa Fluor 488-conjugated goat anti-mouse (ThermoFisher, USA) and Alexa Fluor 555-conjugated anti-rabbit (ThermoFisher, USA) antibodies were used at a dilution 1:50. 4′, 6-diamidino-2-phenylindole (DAPI) stain was used for nuclear staining. Immunofluorescence images were obtained using a Nikon ECLIPSE Ti-S fluorescence microscopy system (Japan).

Statistical analysis

All experiments have been repeated thrice. The results are expressed as means ± SE for the number of indicated determinations. Statistical significance of differences was determined using the Student's unpaired t-test and $p < 0.05$ was considered statistically significant. Analyses were performed using the GraphPad Prism software (GraphPad Software, USA).

Results

Fabrication of ultra-thin PCL nanofiber membrane

The ultra-thin PCL nanofiber membranes were fabricated using electrospinning, followed by transfer to a custom-made 24-well insert as shown in Figure 1(a). The fabrication process of the ultra-thin PCL nanofiber membrane is similar to that described in our previous study.[39] Electrospun PCL nanofibers were produced and placed between two parallel stainless steel plates when a high electrical voltage was applied between the metal needle and the custom-made collector during the ejection of PCL solution. The electrospinning time was set to 30 min to produce a 2-μm-thick ultra-thin nanofiber membrane. As the two edges of the nanofiber membrane were suspended on two parallel stainless steel plates and the center region of the nanofiber membrane was free-standing, the electrospun ultra-thin PCL nanofiber membrane could be transferred easily to the custom-made 24-well insert as shown in Figure 1(b).

Surface immobilization of collagen on ultra-thin PCL nanofiber membrane

Treatment of the ultra-thin PCL nanofiber membrane with NaOH resulted in base hydrolysis of PCL, and the ester linkage of the PCL backbone was converted to carboxyl groups. As a result, the hydrophilicity of the PCL nanofiber membrane increased, which enabled covalent bonding of bioactive compounds such as collagen on the surface of the PCL nanofibers. After the EDC/sulfo-NHS chemical reaction, 2 mg mL^{-1} rat tail collagen type I in the 0.625 M MES buffer solution (pH 6.0) was immobilized on the surface of the PCL nanofibers to increase cell adhesion and viability (Figure 1(c)). The PCL nanofiber membranes before and after collagen immobilization were assessed using SEM. Compared to the original PCL nanofibers (Figure 2(a)), the morphology of the COL-PCL nanofibers (Figure 2(b)) was slightly altered during collagen immobilization. We measured the diameters of the PCL and COL-PCL nanofibers.
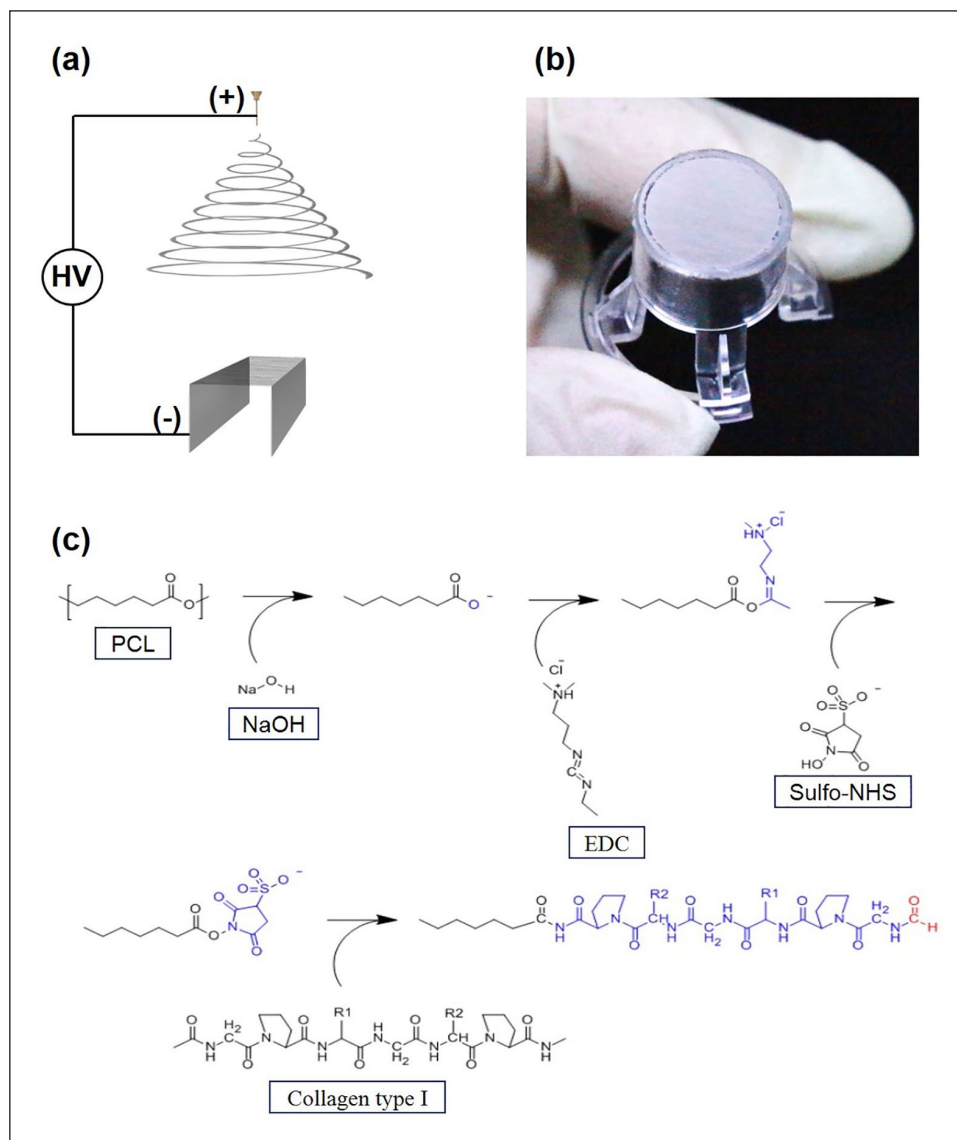
Figure 1. (a) Fabrication process of electrospun ultra-thin nanofibrous membrane insert. (b) Ultra-thin PCL nanofiber membrane on a 24-well insert. (c) Reaction of the base hydrolysis of ester and the immobilization of collagen on ultra-thin nanofiber membrane by EDC/sulfo-NHS chemistry.

Both nanofibers show similar distribution of diameter (Figure 2(c)), although a slight increase in the average diameter of the PCL nanofibers (428 ± 126 nm) was observed compared to the diameter of the COL-PCL nanofibers (498 ± 185 nm). This increase was attributed to collagen immobilization on the surface of the PCL nanofibers. These results implied that collagen type I can be immobilized on the surface of PCL nanofibers.

The contact angles of the PCL and COL-PCL nanofiber membranes are shown in Figure 3(a). The contact angle of the PCL nanofiber membrane was $100 \pm 9.9°$ (Figure 3(b)), whereas that of the COL-PCL nanofiber membrane was $37 \pm 7.3°$ (Figure 3(c)). This demonstrated that the surface immobilization of collagen type 1 via hydrolysis and the EDC/sulfo-NHS reaction on the PCL nanofiber membrane

reduced the contact angle by $\sim 62°$, rendering the PCL nanofiber membrane hydrophilic and suitable for cell adhesion.

To visually confirm the existence of the collagen on the COL-PCL nanofiber membrane, the PCL and COL-PCL nanofiber membrane was stained by aniline blue. As shown in Figure 4, the COL-PCL nanofiber membrane exhibited the blue color due to the presence of the collagen, whereas the PCL nanofiber membrane was not stained by aniline blue. This result confirmed the existence of the collagen in the COL-PCL nanofiber membrane.

To confirm stable collagen immobilization on the PCL nanofibers, the PCL, NaOH-treated PCL, EDC/sulfo-NHS-treated PCL, P-COL-PCL, and COL-PCL nanofiber membranes were analyzed by FTIR spectroscopy. Figure 5 shows
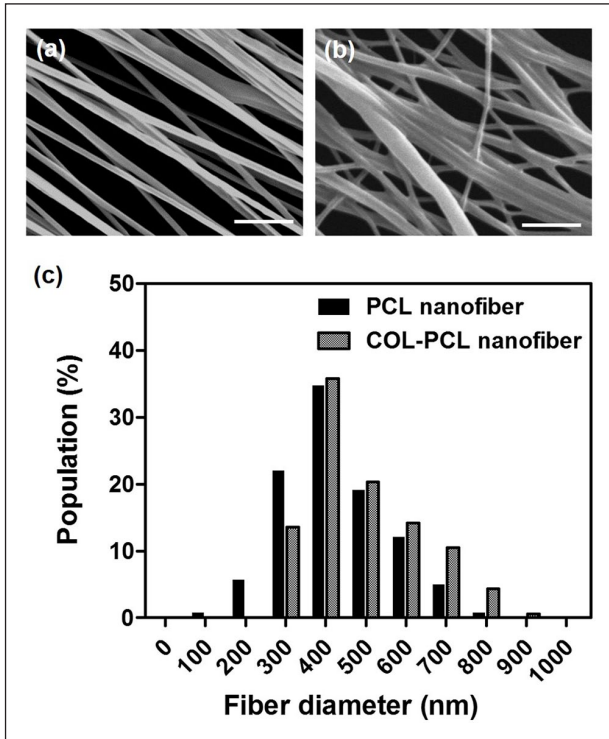
Figure 2. SEM images of a (a) PCL and (b) a COL-PCL nanofiber membrane. (c) The diameter distribution of the PCL and COL-PCL nanofibers.
Scale bars are 10 μm.

Figure 3. Water contact angle measurement of PCL and COL-PCL nanofiber membrane. Photographs of water droplet on the PCL (b) and COL-PCL (c) nanofiber membrane to measure the contact angle.
The values shown are means ± SEs (n = 3). * denotes statistical significance difference (***: p < 0.001) compared to PCL.

the IR spectra of PCL, NaOH-treated PCL, EDC/sulfo-NHS-treated PCL, P-COL-PCL, and COL-PCL nanofiber membranes. The characteristic peaks of PCL due to the ester bonds $(1,729 \, cm)^{-1}$ and CH_2 stretching ($2952 \, cm^{-1}$ for asymmetric and $2868 \, cm^{-1}$ symmetric) were observed for PCL, NaOH-treated PCL, EDC/sulfo-NHS-treated PCL, P-COL-PCL, and COL-PCL nanofiber membranes, indicating that five membranes mainly consisted of PCL nanofibers. After treatment of NaOH and subsequent EDC/sulfo-NHS, the NaOH- and EDC/sulfo-NHS-treated PCL nanofiber membranes showed the additional peak around $3400 \, cm^{-1}$ due to the exposure of OH groups at the terminal, which facilitated the collagen immobilization.[40] After collagen immobilization, the COL-PCL nanofiber membrane showed typical peaks of collagen, including those for amide I ($1658 \, cm^{-1}$), amide II ($1548 \, cm^{-1}$), and amide III ($1238 \, cm^{-1}$), which were not observed in the case of the PCL nanofiber membrane, indicating that collagen was successfully immobilized on the surface of the PCL nanofibers. In contrast, the P-COL-PCL nanofiber membrane showed relatively low characteristic peaks of collagen, which implied that the proposed collagen immobilization process would more efficiently immobilize collagen on the surface of the PCL nanofibers.

Furthermore, the effectiveness and stability of the collagen immobilization process were compared with those
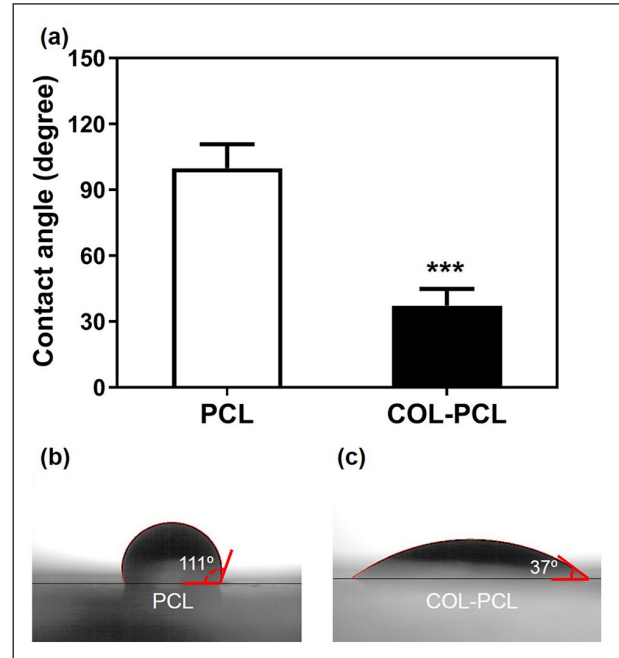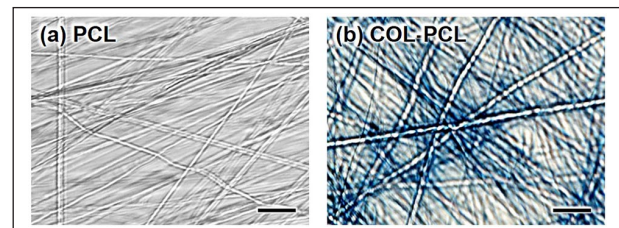

Figure 4. Aniline blue staining image of (a) PCL and (b) COL-PCL nanofiber membrane. Collagen was stained in blue color. Scale bars are 1 μm.

of the physical adsorption of the collagen by TEM. The TEM image of the PCL nanofibers shows a clear interface between the PCL nanofibers and air without collagen (Figure 6(a)). While the TEM images of the P-COL-PCL and COL-PCL nanofibers confirm the existence of the collagen between the PCL nanofibers and air, the amount of the collagen on the surface of the PCL nanofibers shows the great difference (Figure 6(b) and (c)). The TEM images suggested that collagen immobilization provided an abundant and perfect immobilization of collagen on the surface of PCL nanofibers, whereas the physical adsorption of collagen partially and deficiently coated collagen on the surface of the PCL nanofibers.

Biological evaluation of ultra-thin PCL, P-COL-PCL and COL-PCL nanofiber membranes

HUVECs were cultured on the ultra-thin PCL, P-COL-PCL and COL-PCL nanofiber membranes to confirm biocompatibility. After 7 days of cultivation, cell viability on the PCL, P-COL-PCL and COL-PCL nanofiber membranes was compared using the live/dead assay. The COL-PCL nanofiber membrane supported excellent survival ratio of HUVECs ($> 90\%$) for 7 days, and the highest survival rate was 98.0 ± 0.2 on day 5 (Figure 7(a) and (b)). In contrast, the PCL and P-COL-PCL nanofiber membrane showed the highest survival ratio of HUVECs on day 1, which gradually decreased, and eventually all cells died on day 7 (Figure 7(a) and (b)). Therefore, the surface immobilization of collagen can improve the adhesion and viability of cells on the PCL nanofibers.

The expression levels of CD31/PE-CAM, Zo-1, claudin-5, and VE-cadherin in the HUVECs cultured for 7 days were determined to confirm the formation and functioning of the endothelial tight junctions. As shown in Figure 8(a), CD31/PE-CAM, Zo-1, claudin-5, and VE-cadherin were expressed in the HUVECs cultured on the COL-PCL nanofiber membrane, whereas CD31/PE-CAM, Zo-1, and claudin5 were not expressed in the HUVECs on the pristine PCL and P-COL-PCL nanofiber membrane.

A permeability assay was performed using 40 kDa FITC-dextran to study the integrity of HUVECs. Impaired integrity is reflected by an increase in permeability for the 40 kDa FITC-dextran. Results showed that the permeability coefficients of the pristine PCL, COL-PCL and P-COL-PCL nanofiber membrane, and P-COL-PCL and COL-PCL nanofiber membrane with HUVECs were 8.9, 7.0, 8.0, 6.2, and 1.1 cm s,$^{-1}$, respectively (Figure 8(b)). The permeability before and after HUVEC culturing on the COL-PCL nanofiber membrane exhibited a drastic change, indicating that the HUVECs successfully formed an endothelium on the COL-PCL membrane.

TEER values were measured to evaluate the HUVEC monolayer and the formation of tight junctions among the HUVECs. As shown in Figure 8(c), the TEER values of the HUVEC layer on the COL-PCL nanofiber membrane showed high peaks at 46 ± 3 and 45 ± 4 Ω cm^2 on days 5 and 7, respectively. The HUVEC layer on the PCL and P-COL-PCL nanofiber membrane showed lower TEER values than those on the COL-PCL nanofiber membrane (Figure 8(c)). These results demonstrated that the surface immobilization of collagen effectively promoted *in vitro* endothelialization on the ultra-thin PCL nanofiber membrane while maintaining ECM-mimetic nanofiber structure.
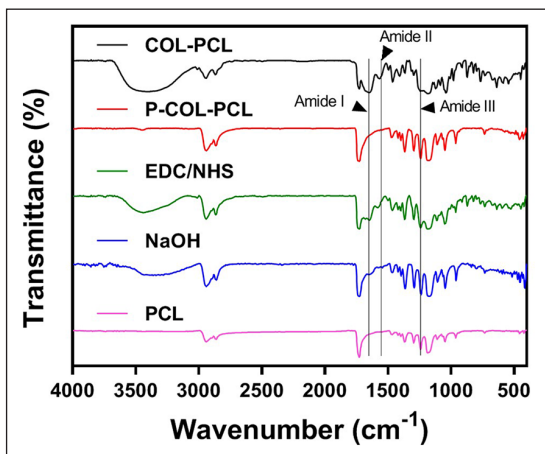
Discussion

PCL is a synthetic polymer widely used in tissue engineering owing to excellent biodegradability, mechanical strength, and non-toxicity. Especially, PCL was approved by FDA for its use as a support for bones and scaffolds,
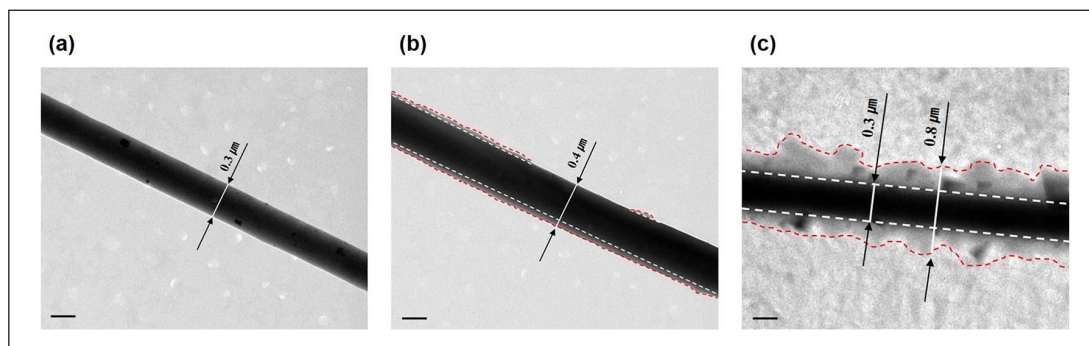

Figure 5. FTIR spectra at wave numbers from 4000 to 500 cm^{-1} of PCL (purple line), NaOH-treated PCL (blue line), EDC/NHS-treated PCL (green line), P-COL-PCL (red line) and COL-PCL nanofiber (black line).

Figure 6. (a) Field emission transmission electron microscope (FE-TEM) images of PCL, (b) P-COL-PCL, and (c) COL-PCL nanofiber.
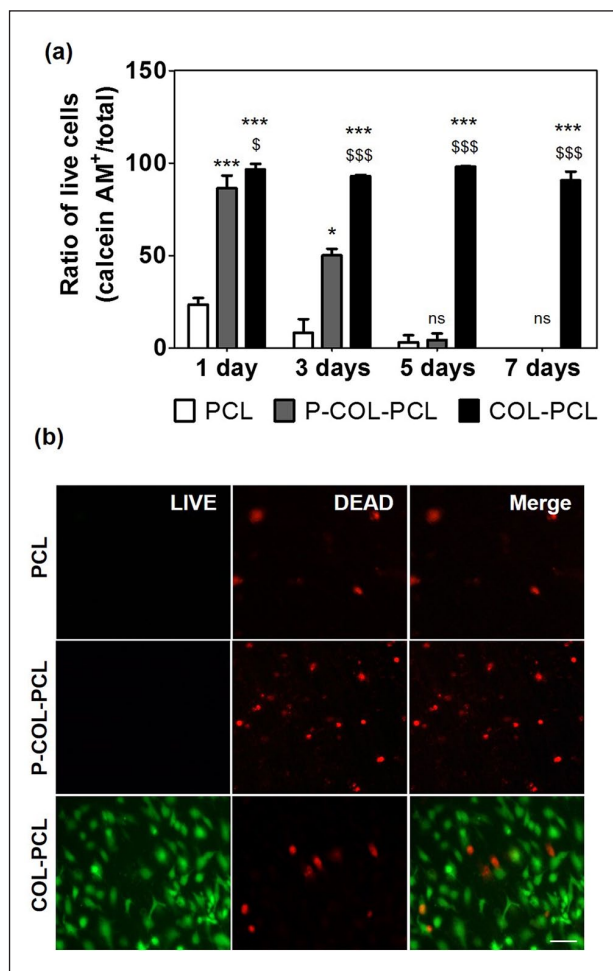Scale bars are 0.2 μm.

Figure 7. LIVE/DEAD assay of HUVECs on the ultra-thin PCL and COL-PCL nanofiber membrane nanofiber membrane. (a) Ratio of live HUVECs on the PCL and COL-PCL nanofiber membrane. The values shown are means ± SEs (n = 3). * and $ denote statistical significance difference (* and $: p < 0.05, *** and $$$: p < 0.001 and ns: not statistically significant) compared to PCL and P-COL-PCL, respectively. (b) Images of the LIVE/DEAD assay of the HUVECs on the PCL and COL-PCL nanofiber membrane (live and dead cells were stained green and red, respectively, at day 7). Scale bars are 100 μm.

and so on, due to its non-toxicity and biodegradability in the human body.[41] However, PCL is hydrophobic, which reduces cell attachment, viability, and proliferation. Therefore, post-processing of PCL nanofibers is essential for increasing its hydrophilicity, which in turn enhances cell adhesion. In this study, we utilized hydrolysis with NaOH, followed by EDC/sulfo-NHS reaction, to improve hydrophilicity and biocompatibility of the PCL nanofibers while maintaining the original nanofiber structure. We fabricated an ultra-thin PCL nanofiber membrane in the form of a Transwell® like insert system, which is a type of *in vitro* cell culture platform for recapitulating the *in vivo* blood vessel-tissue interface. Considering that the thickness of the *in vivo* blood vessel-tissue interface is of

nanometer scale depending on the tissues or organs, we attempted to reduce the thickness of the nanofiber membrane to ~ 2 μm. To maintain the original structure of the ultra-thin PCL nanofiber membrane, a post-processing method that does not adversely affect the PCL nanofibers is required. Although plasma treatment, a well-known post-processing method used in tissue engineering, increases hydrophilicity and cell adhesion, it also generates heat in the sample. The PCL nanofibers are sensitive to heat, and thus, plasma treatment can easily damage its ultra-thin structure. To prevent this thermal damage, a relatively expensive plasma system is necessary to precisely control the plasma power. In contrast, wet chemical methods, including hydrolysis, aminolysis, and wet coating, enabled to functionalize the ultra-thin PCL nanofiber membrane with a low cost, simple and stable way without expensive equipment.[31,42] Instead, we introduced a low cost and simple surface modification method of hydrolysis followed by EDC/sulfo-NHS reaction for immobilizing collagen on the surface of the PCL nanofibers. Surface hydrolysis with bases has been reported to improve surface wettability or create new functions.[31,42] In this study, NaOH treatment generated carboxylate ions in the PCL nanofibers due to hydrolysis of the ester bonds (Figure 1(c)). This functional group not only increased the hydrophilicity, but also provided a means of covalently bonding the bioactive compound to improve cell-material interactions (Figure 5).[43] However, hydrolysis with NaOH can adversely affect the mechanical properties of the ultra-thin PCL nanofiber membrane. In this study, 0.1 M NaOH was used for optimal hydrolysis to minimize adverse effects on the mechanical properties of the PCL nanofiber membrane.[44] Collagen was immobilized on the nanofiber surface via the EDC/sulfo-NHS reaction. Collagen immobilization was confirmed using various methods such as SEM, FTIR, and measurement of the water contact angle.

Collagen immobilization improved the hydrophilicity and biocompatibility of the ultra-thin PCL nanofiber membrane without affecting the nanofiber structure. The structure of PCL nanofibers has played an important role in cell growth and tissue formation owing to its similarity with the structure of native ECM environments.[30,44,45] Therefore, the structure of the PCL nanofiber has to be maintained during the post-processing modification of the nanofiber.[36,42,46] The SEM images confirmed the maintenance of the original structure of PCL nanofibers in the COL-PCL nanofiber membrane (Figure 2(b)), although a slight increase in the diameter of COL-PCL nanofibers, compared to that of the PCL nanofibers, was observed due to the collagen immobilization on the surface of the PCL nanofibers. Furthermore, the hydrophilicity of the ultra-thin PCL nanofiber membrane was dramatically increased after collagen immobilization. The average contact angle of the ultra-thin PCL nanofiber membrane was 100 ± 9.9°,
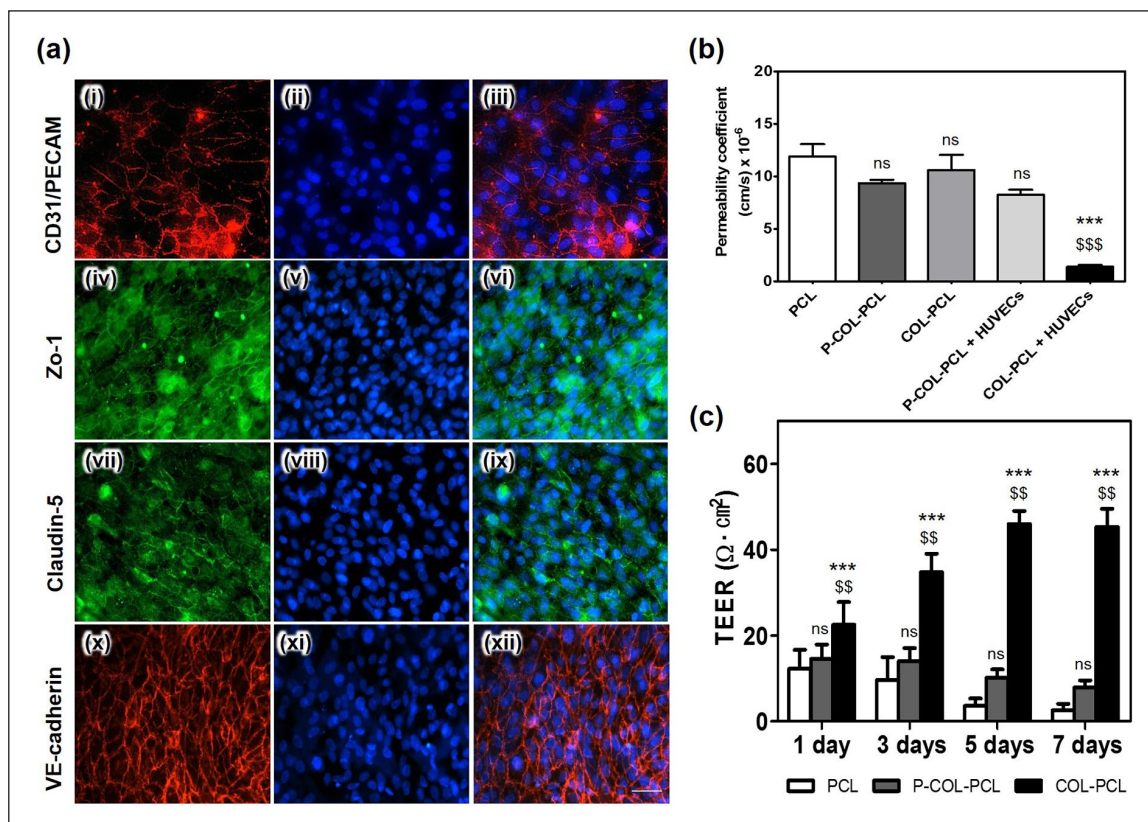
Figure 8. Cell–cell junctions of the HUVECs on the ultra-thin PCL nanofiber membrane surface immobilized with collagen type I (a-(i, iv, vii, x)). Immunofluorescence staining of the junction proteins, CD 31/PECAM (red in a-(i, iii)), VE-cadherin (red in a-(x, xii)), and the tight junction protein Zo-1 (green in a-(iv, vi)) and claudin-5 (green in a-(vii, ix)). Nuclear stain using DAPI (blue in a-(ii, iii, v, vi, viii, ix, xi, xii)). (b) Permeability of the pristine PCL, COL-PCL and P-COL-PCL nanofiber membrane, and P-COL-PCL and COL-PCL nanofiber membrane with HUVECs using 40 kD dextran-FITC. The values shown are means $\pm$ SEs (n = 3). * and $ denote statistical significance difference (*** and $$$: $p < 0.001$ and ns: not statistically significant) compared to PCL and P-COL-PCL, respectively. (c) The measured TEER values of HUVECs on the PCL, P-COL-PCL and COL-PCL nanofiber membrane with respect to cell culture period. The values shown are means $\pm$ SEs (n = 3). * and $ denote statistical significance difference ($$: $p < 0.01$, ***: $p < 0.001$ and ns: not statistically significant) compared to PCL and P-COL-PCL, respectively. Scale bars are 50 μm.

whereas the contact angle of the COL-PCL nanofiber membrane was reduced to $37 \pm 7.3°$ (Figure 3(a)). A low contact angle implied increase in the hydrophilicity of the surface,[44,47] which enhances cell adhesion and viability (Figure 7(a) and (b)). FTIR analysis was used to confirm immobilization of collagen on the surface of the PCL nanofibers. The appearance of the typical peaks of collagen, including those of amide I, II, and III on the COL-PCL nanofiber membrane indicated the presence of collagen on the surface of the PCL nanofibers (Figure 5). The aniline blue staining of the PCL and COL-PCL nanofiber membrane also confirmed the existence of the collagen in the COL-PCL nanofiber membrane. The SEM and FTIR analyses, and aniline blue staining showed collagen immobilization on the surface of the PCL nanofibers without significant alteration of the original structure of the PCL nanofiber. Furthermore, we compared the COL-PCL nanofiber membrane with the P-COL-PCL nanofiber

membrane by the TEM images (Figure 6). Compared with the P-COL-PCL, which has been frequently utilized to improve the biocompatibility, the proposed collagen immobilization process provided more efficient and stable collagen immobilization on the surface of the PCL nanofibers, which demonstrated the benefits of the proposed collagen immobilization process. Furthermore, HUVECs on the COL-PCL nanofiber membrane showed higher viability for 7 days cultures, whereas those on the PCL and P-COL-PCL nanofiber membranes were almost dead after 7 days in culture. Though the physical adsorption process would allow collagen to be coated on the PCL nanofiber membrane, physically adsorbed collagen was known to be readily removed,[48] degraded, or absorbed into intracellular domain.[49] For this reason, the HUVECs on P-COL-PCL showed high viability in the first day, but the viability of the HUVECs was continuously decreased for 7 days. In contrast, HUVECs on the COL-PCL nanofiber membrane

maintained high viability for 7 days in culture, which confirmed the efficiency of the collagen immobilization process.

To assess the long-term homeostasis of cells, TEER, permeability, and the expression of junction protein were identified. TEER measurement has been widely used as a quantitative method for evaluating tight junction function, and integrity and permeability of the endothelial monolayer in cell culture models of the endothelium.[50–53] In addition, junction protein expression is an important indicator of normal vascular endothelial function.[30,54,55] The increase in the TEER value with respect to cull culture period and the expression of CD31, Zo-1, claudin-5, and VE-cadherin confirmed that the endothelial cells were normally cultured and formed tight junctions on the COL-PCL nanofiber membrane in 7 days (Figure 8).[56–58] Thus, the COL-PCL nanofiber membrane had excellent biocompatibility in terms of cell adhesion, viability, permeability, and formation of cell–-cell junction (Figures 7 and 8). In this regard, collagen immobilization improved the cell adhesion and homeostasis of the ultra-thin PCL nanofiber membrane without significantly affecting the nanofiber structure.

Conclusion

A collagen immobilization process on an ultra-thin PCL nanofiber membrane, which involved hydrolysis with NaOH, followed by EDC/sulfo-NHS reaction, was utilized to provide a biocompatible environment for endothelialization on the PCL nanofibers. This process successfully immobilized collagen on the surface of the PCL nanofibers while maintaining the original structure of the membrane. The immobilized collagen promoted endothelialization and maintained the endothelial cell homeostasis by increasing cell attachment, viability, TEER value, and tight junction formation. Therefore, this process is expected to be widely used in tissue engineering and *in vitro* cell culture platforms, which requires recapitulation of blood vessel formation.

Declaration of conflicting interests

The author(s) declared no potential conflicts of interest with respect to the research, authorship, and/or publication of this article.

Funding

ORCID iD

Byeong-ung Park   https://orcid.org/0000-0003-4417-6908

References

1. Holland I, Logan J, Shi J, et al. 3D biofabrication for tubular tissue engineering. *Biodes Manuf* 2018; 1(2): 89–100.
2. Ashammakhi N, Elkhammas E and Hasan A. Translating advances in organ-on-a-chip technology for supporting organs. *J Biomed Mater Res B Appl Biomater* 2019; 107(6): 2006–2018.
3. Ikada Y. Challenges in tissue engineering. *J R Soc Interface* 2006; 3: 589–601.
4. Shevchenko RV, James SL and James SE. A review of tissue-engineered skin bioconstructs available for skin reconstruction. *J R Soc Interface* 2010; 7(43): 229–258.
5. Cao H, Liu T and Chew SY. The application of nanofibrous scaffolds in neural tissue engineering. *Adv Drug Deliv Rev* 2009; 61(12): 1055–1064.
6. Xie J, MacEwan MR, Schwartz AG, et al. Electrospun nanofibers for neural tissue engineering. *Nanoscale* 2010; 2: 35–44.
7. Osakada F, Jin ZB, Hirami Y, et al. In vitro differentiation of retinal cells from human pluripotent stem cells by small-molecule induction. *J Cell Sci* 2009; 122(Pt. 17): 3169–3179.
8. Choi KD, Yu J, Smuga-Otto K, et al. Hematopoietic and endothelial differentiation of human induced pluripotent stem cells. *Stem Cells* 2009; 27(3): 559–567.
9. Sekiya S, Shimizu T, Yamato M, et al. Bioengineered cardiac cell sheet grafts have intrinsic angiogenic potential. *Biochem Biophys Res Commun* 2006; 341(2): 573–582.
10. Masuda S, Shimizu T, Yamato M, et al. Cell sheet engineering for heart tissue repair. *Adv Drug Deliv Rev* 2008; 60(2): 277–285.
11. Huh D, Matthews BD, Mammoto A, et al. Reconstituting organ-level lung functions on a chip. *Science* 2010; 328(5986): 1662–1668.
12. Nakayama Y, Furukoshi M, Terazawa T, et al. Development of long in vivo tissue-engineered "Biotube" vascular grafts. *Biomaterials* 2018; 185: 232–239.
13. Cheng A, Schwartz Z, Kahn A, et al. Advances in porous scaffold design for bone and cartilage tissue engineering and regeneration. *Tiss Eng Part B Rev* 2018; 25: 14–29.
14. Muzzarelli RA, El Mehtedi M, Bottegoni C, et al. Genipin-crosslinked chitosan gels and scaffolds for tissue engineering and regeneration of cartilage and bone. *Mar Drugs* 2015; 13(12): 7314–7338.
15. Trachtenberg JE, Vo TN and Mikos AG. Pre-clinical characterization of tissue engineering constructs for bone and cartilage regeneration. *Ann Biomed Eng* 2015; 43(3): 681–696.
16. Ebrahimkhani MR, Young CL, Lauffenburger DA, et al. Approaches to in vitro tissue regeneration with application for human disease modeling and drug development. *Drug Discov Today* 2014; 19(6): 754–762.
17. Park SM, Eom S, Hong H, et al. Reconstruction of in vivo-like in vitro model: enabling technologies of microfluidic systems for dynamic biochemical/mechanical stimuli. *Microelectronic Engineering* 2019; 203–204: 6–24.

18. Pittenger MF, Mackay AM, Beck SC, et al. Multilineage potential of adult human mesenchymal stem cells. *Science* 1999; 284(5411): 143–147.

19. Schaffler A and Buchler C. Concise review: adipose tissue-derived stromal cells–basic and clinical implications for novel cell-based therapies. *Stem Cells* 2007; 25(4): 818–827.

20. Blais M, Parenteau-Bareil R, Cadau S, et al. Concise review: tissue-engineered skin and nerve regeneration in burn treatment. *Stem Cells Transl Med* 2013; 2(7): 545–551.

21. Kim S, Lee H, Chung M, et al. Engineering of functional, perfusable 3D microvascular networks on a chip. *Lab Chip* 2013; 13(8): 1489–1500.

22. Carmeliet P and Jain RK. Principles and mechanisms of vessel normalization for cancer and other angiogenic diseases. *Nat Rev Drug Discov* 2011; 10(6): 417–427.

23. He W, Yong T, Teo WE, et al. Fabrication and endothelialization of collagen-blended biodegradable polymer nanofibers: potential vascular graft for blood vessel tissue engineering. *Tissue Eng* 2005; 11(9–10): 1574–1588.

24. Li Y, Li X, Zhao R, et al. Enhanced adhesion and proliferation of human umbilical vein endothelial cells on conductive PANI-PCL fiber scaffold by electrical stimulation. *Mater Sci Eng C Mater Biol Appl* 2017; 72: 106–112.

25. Bose S, Robertson SF and Bandyopadhyay A. Surface modification of biomaterials and biomedical devices using additive manufacturing. *Acta Biomater* 2018; 66: 6–22.

26. Theocharis AD, Skandalis SS, Gialeli C, et al. Extracellular matrix structure. *Adv Drug Deliv Rev* 2016; 97: 4–27.

27. Zamani R, Aval SF, Pilehvar-Soltanahmadi Y, et al. Recent advances in cell electrospining of natural and synthetic nanofibers for regenerative medicine. *Drug Res* 2018; 68(8): 425–435.

28. Chung M, Ahn J, Son K, et al. Biomimetic model of tumor microenvironment on microfluidic platform. *Adv Healthc Mater* 2017; 6(15). DOI: 10.1002/adhm.201700196.

29. Clause KC and Barker TH. Extracellular matrix signaling in morphogenesis and repair. *Curr Opin Biotechnol* 2013; 24(5): 830–833.

30. Kang D, Kim JH, Jeong YH, et al. Endothelial monolayers on collagen-coated nanofibrous membranes: cell-cell and cell-ECM interactions. *Biofabrication* 2016; 8(2): 025008. DOI: 10.1088/1758-5090/8/2/025008.

31. Zhu Y, Gao C, Liu X, et al. Surface modification of polycaprolactone membrane via aminolysis and biomacromolecule immobilization for promoting cytocompatibility of human endothelial cells. *Biomacromolecules* 2002; 3(6): 1312–1319.

32. Zonari A, Novikoff S, Electo NR, et al. Endothelial differentiation of human stem cells seeded onto electrospun polyhydroxybutyrate/polyhydroxybutyrate-co-hydroxyvalerate fiber mesh. *Plos One* 2012; 7(4): e35422.

33. Binulal NS, Natarajan A, Menon D, et al. Gelatin nanoparticles loaded poly(epsilon-caprolactone) nanofibrous semisynthetic scaffolds for bone tissue engineering. *Biomed Mater* 2012; 7(6): 065001.

34. Place ES, George JH, Williams CK, et al. Synthetic polymer scaffolds for tissue engineering. *Chem Soc Rev* 2009; 38: 1139–1151.

35. Ma Z, Mao Z and Gao C. Surface modification and property analysis of biomedical polymers used for tissue engineering. *Colloids Surf B Biointerfaces* 2007; 60(2): 137–157.

36. Yoo HS, Kim TG and Park TG. Surface-functionalized electrospun nanofibers for tissue engineering and drug delivery. *Adv Drug Deliv Rev* 2009; 61(12): 1033–1042.

37. Park SM and Kim DS. Electrolyte-assisted electrospinning for a self-assembled, free-standing nanofiber membrane on a curved surface. *Adv Mater* 2015; 27(10): 1682–1687.

38. Park SM, Kim H, Song KH, et al. Ultra-thin, aligned, free-standing nanofiber membranes to recapitulate multi-layered blood vessel/tissue interface for leukocyte infiltration study. *Biomaterials* 2018; 169: 22–34.

39. Park SM, Lee K-p, Huh M-I, et al. Development of an in vitro 3D choroidal neovascularization model using chemically induced hypoxia on an ultra-thin, free-standing nanofiber membrane. *Mater Sci Eng Pt C* 2018; 104: 109964.

40. Liverani L, Killian MS and Boccaccini AR. Fibronectin functionalized electrospun fibers by using benign solvents: best way to achieve effective functionalization. *Front Bioeng Biotechnol* 2019; 7: 68.

41. Woodruff MA and Hutmacher DW. The return of a forgotten polymer—polycaprolactone in the 21st century. *Prog Polym Sci* 2010; 35: 1217–1256.

42. Croll TI, O'Connor AJ, Stevens GW, et al. Controllable surface modification of poly(lactic-co-glycolic acid) (PLGA) by hydrolysis or aminolysis I: physical, chemical, and theoretical aspects. *Biomacromolecules* 2004; 5(2): 463–473.

43. Jafari-Sabet M, Nasiri H and Ataee R. The effect of cross-linking agents and collagen concentrations on properties of collagen scaffolds. *J Arch Mil Med* 2016; 4: e42367.

44. Sadeghi AR, Nokhasteh S, Molavi AM, et al. Surface modification of electrospun PLGA scaffold with collagen for bioengineered skin substitutes. *Mater Sci Eng C Mater Biol Appl* 2016; 66: 130–137.

45. Bettinger CJ, Langer R and Borenstein JT. Engineering substrate topography at the micro- and nanoscale to control cell function. *Angew Chem Int Ed Engl* 2009; 48(30): 5406–5415.

46. Barnes CP, Pemble CW, Brand DD, et al. Cross-linking electrospun type II collagen tissue engineering scaffolds with carbodiimide in ethanol. *Tissue Eng* 2007; 13(7): 1593–1605.

47. Fu W, Liu Z, Feng B, et al. Electrospun gelatin/PCL and collagen/PLCL scaffolds for vascular tissue engineering. *Int J Nanomedicine* 2014; 9: 2335–2344.

48. Cheng Z and Teoh SH. Surface modification of ultra thin poly (epsilon-caprolactone) films using acrylic acid and collagen. *Biomaterials* 2004; 25(11): 1991–2001.

49. Heo Y, Shin YM, Lee YB, et al. Effect of immobilized collagen type IV on biological properties of endothelial cells for the enhanced endothelialization of synthetic vascular graft materials. *Colloids Surf B Biointerfaces* 2015; 134: 196–203.

50. Srinivasan B, Kolli AR, Esch MB, et al. TEER measurement techniques for in vitro barrier model systems. *J Lab Autom* 2015; 20(2): 107–126.

51. Maheraly Z, Fillmore HL, Tan SL, et al. Real-time acquisition of transendothelial electrical resistance in an all-human,

in vitro, 3-dimensional, blood-brain barrier model exemplifies tight-junction integrity. *FASEB J* 2018; 32(1): 168–182.

52. Ferrell N, Desai RR, Fleischman AJ, et al. A microfluidic bioreactor with integrated transepithelial electrical resistance (TEER) measurement electrodes for evaluation of renal epithelial cells. *Biotechnol Bioeng* 2010; 107(4): 707–716.

53. Lippmann ES, Azarin SM, Kay JE, et al. Derivation of blood-brain barrier endothelial cells from human pluripotent stem cells. *Nat Biotechnol* 2012; 30(8): 783–791.

54. Privratsky JR and Newman PJ. PECAM-1: regulator of endothelial junctional integrity. *Cell Tissue Res* 2014; 355(3): 607–619.

55. Joner M, Nakazawa G, Finn AV, et al. Endothelial cell recovery between comparator polymer-based drug-eluting stents. *J Am Coll Cardiol* 2008; 52(5): 333–342.

56. de Vries HE, Blom-Roosemalen MC, van Oosten M, et al. The influence of cytokines on the integrity of the blood-brain barrier in vitro. *J Neuroimmunol* 1996; 64(1): 37–43.

57. Abbott NJ, Ronnback L and Hansson E. Astrocyte-endothelial interactions at the blood-brain barrier. *Nat Rev Neurosci* 2006; 7: 41–53.

58. Eom S, Park SM, Han SJ, et al. One-step fabrication of a tunable nanofibrous well insert via electrolyte-assisted electrospinning. *RSC Advances* 2017; 7: 38300–38306.